JOURNAL OF SOLID STATE CHEMISTRY **30**, 283–292 (1979)

Phase Relations and Thermodynamics of Nonstoichiometric Vanadium Sulfide in the Range VS through V_3S_4

M. NAKANO-ONODA

National Institute for Researches in Inorganic Materials, 1-1 Namiki, Sakura-Mura, Niihari-Gun, Ibaraki, Japan

AND M. NAKAHIRA

Okayama College of Science, Laboratory for Solid State Chemistry, 1-1 Ridai-Cho, Okayama, Japan

Received September 20, 1978

The composition–equilibrium sulfur pressure relation at 750 through 1217°C in the range VS through V_3S_4 was determined by using an H_2–H_2S technique. At temperatures above 888°C a horizontal part in the P_{S_2}–composition isothermal line was observed, which indicated the existence of a two-phase region. At low temperatures, however, it was not recognized. A statistical thermodynamical treatment which started with the V_3S_4-type model was attempted by considering three kinds of interaction energies. Qualitative trends of the experimental results at the temperatures above 888°C were interpreted on the basis of the discussed model.

Introduction

Previous investigations on the phase relations of nonstoichiometric vanadium sulfide were performed mainly by X-ray study on samples synthesized in an evacuated silica tube at temperatures near 800°C (*1, 2*). In those cases, X-ray studies were made of quenched specimens made by various quenching processes, and inconsistent results were obtained between different investigators. The temperature dependence of the phase relation was not found. Recently Shibata (*3*) and Wakihara *et al.* (*4*) studied the V–S system in the range V_3S_4 through V_5S_8 by determining the composition–equilibrium sulfur pressure isotherm at temperatures below 927°C. However, information relating to the phase equilibrium of the system is still limited.

Many researches concerning the crystal structure of vanadium sulfide were performed (*2, 5–9*) and the structures of representative compounds such as V_3S_4 and V_5S_8 were determined. Further, several results of experiments have been reported and discussed regarding the order–disorder transition of the vanadium vacancies in the V–S system (*10–12*). Nevertheless, the structure and the phase transition have not been well correlated to the phase diagram.

In the present work the composition–equilibrium sulfur pressure relations at 750 through 1217°C in the range VS through V_3S_4 were determined by using an H_2–H_2S technique. A statistical thermodynamical treatment was attempted to interpret the experimental results and to clarify the characteristics of the phase relation in the V–S system.

0022-4596/79/120283-10$02.00/0

Experimental

A starting sulfide, $V_{0.714}S$, was prepared from $VOSO_4 \cdot 3H_2O$ by heating in a stream of H_2S at 1000°C for several hours. Another starting sulfide, $V_{0.909}S$, was prepared by reducing $V_{0.714}S$ in a stream of H_2 containing 0.06% H_2S at 1217°C. The control of equilibrium sulfur pressure was realized by use of gas mixtures of H_2S and H_2. The ratio of H_2S to H_2 was regulated in the range of about 10^{-6} to 10^2 by a method similar to that used by Darken and Gurry (*13*). The mixture of H_2S and H_2 was again diluted with H_2 for small ratios of H_2S to H_2 (less than 1 to 1000).

Vanadium sulfide was equilibrated with the controlled sulfur pressure in the apparatus shown in Fig. 1. The temperatures used were between 750 and 1217°C. After heating for a sufficient period (about 4 hr for 1217°C and 50 hr for 750°C) the specimen was quenched by moving it to the water cooling position by use of a magnet and an iron piece. The sample was taken out of the apparatus after the atmosphere was replaced by N_2. The quenched samples were identified by powder X-ray diffraction patterns (Ni-filtered Cu $K\alpha$) and the lattice constants were measured. The composition of the sample was determined by weight loss on oxidation to V_2O_5 in air at 500°C (*9*). The precision of the composition for a 200-mg sample was within 0.1%. Sometimes two different experiments were performed under the same conditions by starting with $V_{0.909}S$ as well as $V_{0.714}S$. The compositions of the samples obtained in such runs agreed with one another, confirming that equilibrium was established. Comparison of some results with those obtained by the quartz-spring thermobalance method carried out by Shibata (*3*) below 950°C revealed that little change in the chemical composition took place during quenching.

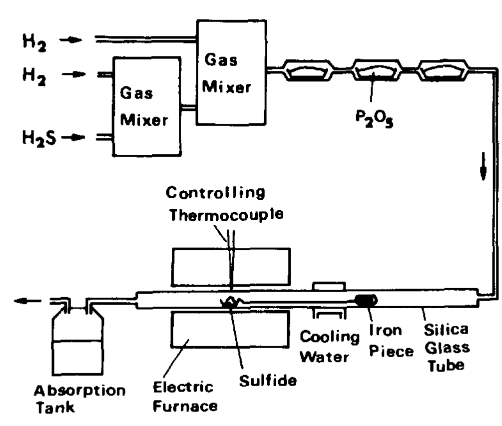

FIG. 1. Apparatus for attaining equilibrium.

Results and Discussion

The value of the equilibrium sulfur pressure was calculated from the mixing ratio of H_2S and H_2 and the reaction temperature by use of thermodynamical data listed in the JANAF thermochemical tables (*14*). The equilibrium sulfur pressures and the composition of the resulting sulfides are shown in Fig. 2 for each temperature. In the range 888 through 1100°C, horizontal parts in the P_{S_2}–composition isothermal lines are observed, indicating the existence of two-phase regions. At 1217°C the phase boundary seems to lie in the vicinity of $V_{0.775}S$. At 827 and 750°C the existence of the two-phase region was not recognized and the composition varied gradually with the equilibrium sulfur pressure.

Powder X-ray diffraction patterns of the quenched samples whose compositions were richer in sulfur than $V_{0.847}S$ could be indexed on the basis of a V_3S_4-type monoclinic unit cell which was described in space group $I2/m$ (C_{2h}^3) (*8*), regardless of the equilibrating temperature. The samples ranging in composition from $V_{0.935}S$ to $V_{0.847}S$ gave powder patterns of the NiAs-type hexagonal cell. The samples whose compositions were richer in vanadium than $V_{0.935}S$ gave powder patterns of the MnP-type orthorhombic cell. Lattice constants obtained for each sulfide were dependent only on the composition,

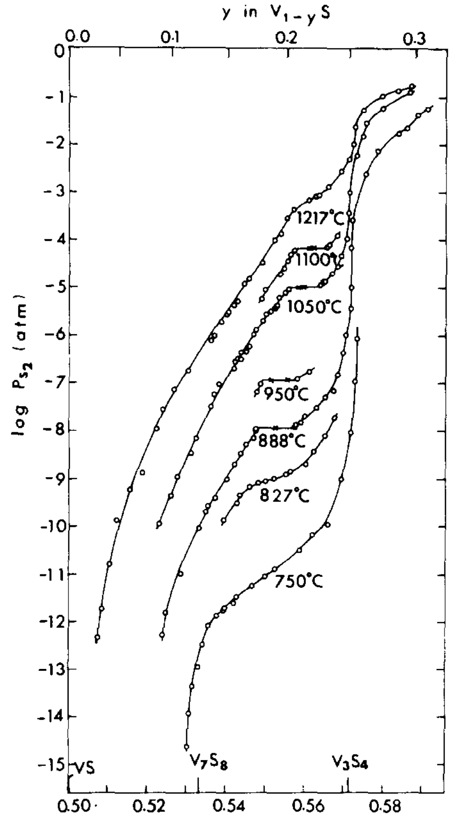

FIG. 2. Equilibrium sulfur pressure (atm)–composition isothermal lines obtained experimentally.

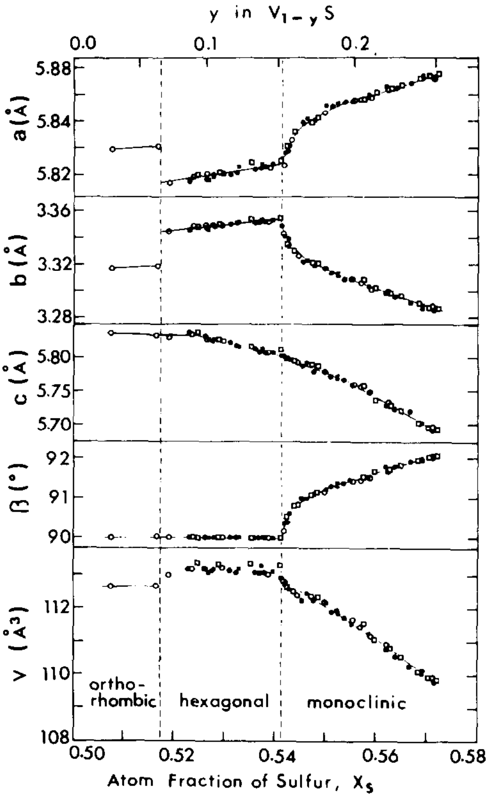

FIG. 3. Lattice constants and volumes of the NiAs–CdI_2 subcells (pseudo-orthohexagonal) in the VS–V_3S_4 range. The equilibrating temperatures are as follows: ○, 1217°C; ●, 1050°C; □, 888°C; ■, 750°C.

and they were almost independent of the temperature from which the sample was quenched. The lattice constants and the volume reduced to the NiAs–CdI_2-type subcell (pseudo-orthohexagonal) of vanadium sulfide are shown in Fig. 3. Specimens within the two-phase region were mixtures of two different monoclinic sulfides. From the lattice constant measurements, the compositions of these sulfides were judged to be those of the two ends of the horizontal line. In view of the change of lattice constants, the monoclinic range illustrated in Fig. 3 seemed to be partitioned into two parts by a composition near $V_{0.79}S$.

Summarizing the above observations:

1. At temperatures above 888°C the existence of a two-phase region was observed. On the other hand at low temperatures it was not recognized.

2. The quenched sample containing more sulfur than $V_{0.847}S$ had the monoclinic $I2/m$ (C_{2h}^3) structure, regardless of whether the existence of the two-phase region was recognized or not.

3. The change of lattice constants of the quenched sample seemed to suggest two kinds of monoclinic lattice. An attempt to interpret these observations consistently was accompanied by considerable difficulty. As the composition is changed from VS toward VS_2, vanadium vacancies are produced in the basic structure of a NiAs type. The vacancies tend to be located in the alternate metal layers and to be ordered in those layers at low

temperatures. Thus structures of various phases are formed. Throughout these structures, however, the constituent layers of different structures are very similar to each other. Such a resemblance may cause complexity in the process of different phase formation especially at low temperatures, and it is not easy to interpret the observations. In this paper, therefore, our consideration is focused on the possibility of a two-phase region between the phases whose compositions are near $V_{0.75}S$ and near VS, respectively.

A statistical thermodynamical treatment which starts with the V_3S_4-type model is attempted. The vacant or occupied octahedral sites of the V_3S_4-type structure may be classified into three types designated as A, B, and C as shown in Fig. 4 and the vanadium occupancy ratios for these sites are represented by a, b, and c, respectively. The following relation is expected to hold for the V_3S_4-type structure;

$$a < b, \qquad c \approx 1.$$

As special cases, the NiAs-type structure and the CdI_2-type structure may be treated on the basis of the same classification as the octahedral sites as given below.

$$a = b = c \leqslant 1 \qquad \text{(for NiAs type)},$$

and

$$a = b < 1, \qquad c \approx 1 \qquad \text{(for CdI}_2\text{ type)}.$$

The grand partition function of this system is given by

(G.P.F.)

$$= \sum \frac{(N/4)!}{N_A!\,(N/4-N_A)!}\,\frac{(N/4)!}{N_B!\,(N/4-N_B)!} \times \frac{(N/2)!}{N_C!\,(N/2-N_C)!}\,\frac{N!}{N_S!\,(N-N_S)!} \times [\lambda_V q_V(T)]^{N_A+N_B+N_C}[\lambda_S q_S(T)]^{N_S} \exp\left(-\frac{E}{kT}\right). \tag{1}$$

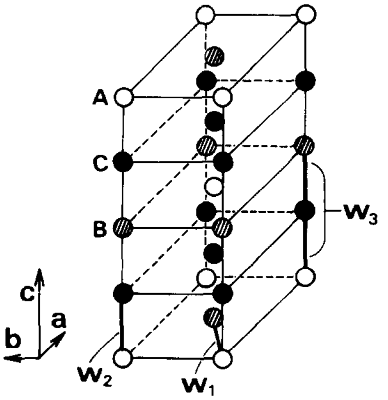

FIG. 4. Crystal structure of the V_3S_4 type. The sulfur layers are eliminated. The octahedral sites are classified into three types, A, B, and C. w_1, w_2, and w_3 are the pairwise interaction energies (see text).

N is the number of sulfur sites and is equal to the sum of octahedral sites. N_A, N_B, and N_C are the number of vanadium ions on A, B, and C sites and N_S is the number of sulfur ions. λ_V and λ_S are the absolute activities of vanadium and sulfur ions, respectively. It is assumed as an approximation that the partition functions of the lattice vibration of vanadium ions of the A, B, and C sites are equal; then $q_V(T)$ and $q_S(T)$ are the partition functions of the lattice vibration of vanadium and sulfur ions, respectively. E is the potential energy of the lattice configurations which may be expressed by

$$E = \{N - (N_A + N_B + N_C)\}\varepsilon_V + (N - N_S)\varepsilon_S + \sum \varepsilon_{jk} n_{jk} \tag{2}$$

where ε_i ($i = \text{V, S}$) is the energy required to remove an ion of the species i from an internal lattice point to a new surface lattice point, leaving a vacancy. ε_{jk} ($j, k = A, B, C, \text{S}$) is the interaction energy between the vacancies situated in sites A, B, C or in the sulfur sites; ε_{jk} includes Z_{jk} which is the number of the neighboring sites of k species around j species. n_{jk} is the number of the vacancy pair of j-k.

Writing Eq. (1) as (G.P.F.) = $\sum$ (term), the equilibrium conditions are given by the following equations:

$$0=\frac{\partial \ln(\text{term})}{\partial N_A}$$
$$\doteqdot \ln\frac{N/4-N_A}{N_A}+\ln[\lambda_V q_V(T)]-\frac{1}{kT}\frac{\partial E}{\partial N_A}, \tag{3}$$

$$0=\frac{\partial \ln(\text{term})}{\partial N_B}$$
$$\doteqdot \ln\frac{N/4-N_B}{N_B}+\ln[\lambda_V q_V(T)]-\frac{1}{kT}\frac{\partial E}{\partial N_B}, \tag{4}$$

$$0=\frac{\partial \ln(\text{term})}{\partial N_C}$$
$$\doteqdot \ln\frac{N/2-N_C}{N_C}+\ln[\lambda_V q_V(T)]-\frac{1}{kT}\frac{\partial E}{\partial N_C} \tag{5}$$

$$0=\frac{\partial \ln(\text{term})}{\partial N_S}$$
$$\doteqdot \ln\frac{N-N_S}{N_S}+\ln[\lambda_S q_S(T)]-\frac{1}{kT}\frac{\partial E}{\partial N_S}, \tag{6}$$

$$0=\frac{\partial \ln(\text{term})}{\partial N}$$
$$\doteqdot \frac{1}{4}\ln\frac{N/4}{N/4-N_A}+\frac{1}{4}\ln\frac{N/4}{N/4-N_B}$$
$$+\frac{1}{2}\ln\frac{N/2}{N/2-N_C}+\ln\frac{N}{N-N_S}-\frac{1}{kT}\frac{\partial E}{\partial N}. \tag{7}$$

The Bragg–Williams approximation is adopted as shown in Table I. $\partial E/\partial N_A$, $\partial E/\partial N_B$, $\partial E/\partial N_C$, $\partial E/\partial N_S$, or $\partial E/\partial N$ is the sum of the differentiated terms given in the vertical columns of Table I. Three kinds of vanadium vacancy pairs are taken into account. One is the first-nearest neighbor in the metal layer, and the other two are the first- and second-nearest neighbors normal to the layer. The pairwise interaction energies between those neighboring vacancies are designated as w_1, w_2, and w_3 as shown in Fig. 4. Counting the number of these pairs in the V_3S_4-type structure, it may be assumed that the following relations hold approximately:

$$\begin{aligned}
&\varepsilon_{AA}=2w_1, \qquad \varepsilon_{AB}=4w_1+2w_3,\\
&\varepsilon_{AC}=2w_2;\\
&\varepsilon_{BB}=2w_1, \qquad \varepsilon_{BC}=2w_2,\\
&\varepsilon_{CC}=6w_1+2w_3.
\end{aligned} \tag{8}$$

It may be assumed that the interaction energy between vanadium and sulfur vacancies does not depend on the kind of vanadium site; then

$$\varepsilon_{AS}=\varepsilon_{BS}=\varepsilon_{CS}. \tag{9}$$

In the present work, the sulfur vacancies were not taken into account. The following equations were obtained by eliminating $\ln(N-N_S)$ from Eqs. (6) and (7) and using the relation $N=N_S$.

$$\ln\frac{N_S/4-N_A}{N_A}+\ln[\lambda_V q_V(T)]-\frac{1}{kT}\frac{\partial E}{\partial N_A}=0, \tag{3$'$}$$

$$\ln\frac{N_S/4-N_B}{N_B}+\ln[\lambda_V q_V(T)]-\frac{1}{kT}\frac{\partial E}{\partial N_B}=0, \tag{4$'$}$$

$$\ln\frac{N_s/2-N_C}{N_C}+\ln[\lambda_V q_V(T)]-\frac{1}{kT}\frac{\partial E}{\partial N_C}=0, \tag{5$'$}$$

and

$$\frac{1}{4}\ln\left[\frac{N_S/4}{N_S/4-N_A}\,\frac{N_S/4}{N_S/4-N_B}\left(\frac{N_S/2}{N_S/2-N_C}\right)^2\right]$$
$$+\ln[\lambda_S q_S(T)]-\frac{1}{kT}\left(\frac{\partial E}{\partial N_S}+\frac{\partial E}{\partial N}\right)=0. \tag{6$'$}$$

Calculating Eq. (3′) − Eq. (4′) and Eq. (3′) + Eq. (4′) − 2 × Eq. (5′), we have

$$\ln\left[\frac{a}{1-a}\,\frac{1-b}{b}\right]-\frac{2(w_1+w_3)}{kT}(a-b)=0, \tag{10}$$

TABLE I

POTENTIAL ENERGY OF LATTICE CONFIGURATIONS OF V_3S_4TYPE (BRAGG-WILLIAMS APPROXIMATION)

$E=\sum(\varepsilon_i n_i+\varepsilon_{jk}n_{jk})$

ε	n	$\partial(\varepsilon n)/\partial N_A$	$\partial(\varepsilon n)/\partial N_B$	$\partial(\varepsilon n)/\partial N_C$	$\partial(\varepsilon n)/\partial N_S$	$\partial(\varepsilon n)/\partial N$
ε_V	$N-(N_A+N_B+N_C)$	$-\varepsilon_V$	$-\varepsilon_V$	$-\varepsilon_V$	0	ε_V
ε_S	$N-N_S$	0	0	0	$-\varepsilon_S$	ε_S
ε_{AA}	$\frac{1}{2}\left(\frac{N}{4}-N_A\right)^2\Big/\left(\frac{N}{4}\right)$	$-\left(1-\frac{N_A}{N/4}\right)\varepsilon_{AA}$	0	0	0	$\frac{1}{8}\left\{1-\left(\frac{N_A}{N/4}\right)^2\right\}\varepsilon_{AA}$
ε_{AB}	$\left(\frac{N}{4}-N_A\right)\left(\frac{N}{4}-N_B\right)\Big/\left(\frac{N}{4}\right)$	$-\left(1-\frac{N_B}{N/4}\right)\varepsilon_{AB}$	$-\left(1-\frac{N_A}{N/4}\right)\varepsilon_{AB}$	0	0	$\frac{1}{4}\left\{1-\frac{N_AN_B}{(N/4)^2}\right\}\varepsilon_{AB}$
ε_{AC}	$\left(\frac{N}{4}-N_A\right)\left(\frac{N}{2}-N_C\right)\Big/\left(\frac{N}{2}\right)$	$-\left(1-\frac{N_C}{N/2}\right)\varepsilon_{AC}$	0	$-\frac{1}{2}\left(1-\frac{N_A}{N/4}\right)\varepsilon_{AC}$	0	$\frac{1}{4}\left\{1-\frac{N_AN_C}{(N/4)(N/2)}\right\}\varepsilon_{AC}$
ε_{BB}	$\frac{1}{2}\left(\frac{N}{4}-N_B\right)^2\Big/\left(\frac{N}{4}\right)$	0	$-\left(1-\frac{N_B}{N/4}\right)\varepsilon_{BB}$	0	0	$\frac{1}{8}\left\{1-\left(\frac{N_B}{N/4}\right)^2\right\}\varepsilon_{BB}$
ε_{BC}	$\left(\frac{N}{4}-N_B\right)\left(\frac{N}{2}-N_C\right)\Big/\left(\frac{N}{2}\right)$	0	$-\left(1-\frac{N_C}{N/2}\right)\varepsilon_{BC}$	$-\frac{1}{2}\left(1-\frac{N_B}{N/4}\right)\varepsilon_{BC}$	0	$\frac{1}{4}\left\{1-\frac{N_BN_C}{(N/4)(N/2)}\right\}\varepsilon_{BC}$
ε_{CC}	$\frac{1}{2}\left(\frac{N}{2}-N_C\right)^2\Big/\left(\frac{N}{2}\right)$	0	0	$-\left(1-\frac{N_C}{N/2}\right)\varepsilon_{CC}$	0	$\frac{1}{4}\left\{1-\left(\frac{N_C}{N/2}\right)^2\right\}\varepsilon_{CC}$
ε_{AS}	$\left(\frac{N}{4}-N_A\right)(N-N_S)/N$	$-\left(1-\frac{N_S}{N}\right)\varepsilon_{AS}$	0	0	$-\frac{1}{4}\left(1-\frac{N_A}{N/4}\right)\varepsilon_{AS}$	$\frac{1}{4}\left\{1-\frac{N_AN_S}{(N/4)N}\right\}\varepsilon_{AS}$
ε_{BS}	$\left(\frac{N}{4}-N_B\right)(N-N_S)/N$	0	$-\left(1-\frac{N_S}{N}\right)\varepsilon_{BS}$	0	$-\frac{1}{4}\left(1-\frac{N_B}{N/4}\right)\varepsilon_{BS}$	$\frac{1}{4}\left\{1-\frac{N_BN_S}{(N/4)N}\right\}\varepsilon_{BS}$
ε_{CS}	$\left(\frac{N}{2}-N_C\right)(N-N_S)/N$	0	0	$-\left(1-\frac{N_S}{N}\right)\varepsilon_{CS}$	$-\frac{1}{2}\left(1-\frac{N_C}{N/2}\right)\varepsilon_{CS}$	$\frac{1}{2}\left\{1-\frac{N_CN_S}{(N/2)N}\right\}\varepsilon_{CS}$
ε_{SS}	$\frac{1}{2}(N-N_S)^2/N$	0	0	0	$-\left(1-\frac{N_S}{N}\right)\varepsilon_{SS}$	$\frac{1}{2}\left\{1-\left(\frac{N_S}{N}\right)^2\right\}\varepsilon_{SS}$
Total		$\partial E/\partial N_A$	$\partial E/\partial N_B$	$\partial E/\partial N_C$	$\partial E/\partial N_S$	$\partial E/\partial N$

$$\ln\left[\frac{a}{1-a}\,\frac{b}{1-b}\left(\frac{1-c}{c}\right)^2\right] - \frac{2(w_2-3w_1-w_3)}{kT}(a+b-2c)=0 \qquad (11)$$

where the relations

$$a=\frac{N_A}{N/4}\doteqdot\frac{N_A}{N_S/4},\quad b=\frac{N_B}{N/4}\doteqdot\frac{N_B}{N_S/4},$$
$$c=\frac{N_C}{N/2}\doteqdot\frac{N_C}{N_S/2} \qquad (12)$$

and the relations expressed by Eq. (8), Eq. (9), and Table I are employed. When the composition of vanadium sulfide is represented by an atom fraction of sulfur X_S or y in $V_{1-y}S$, the following relations between X_S, y, and the occupancy ratios, a, b, and c, hold:

$$\frac{1-X_S}{X_S}=1-y=\frac{a+b+2c}{4}. \qquad (13)$$

By specifying the values of the pairwise interaction energies, w_1, w_2, and w_3, and the temperature for Eqs. (10), (11), and (13), the equilibrium occupancy ratios, a, b, and c, were numerically solved with respect to X_S or y using a computer (FACOM-270-20) in a manner similar to that reported by Oka *et al.* (*12*) and Koiwa and Hirabayashi (*15*).

By using the relation

$$kT\ln\lambda_S=\mu_S=\mu^\circ_S(T)+kT\ln P_{S_2}^{1/2}, \qquad (14)$$

one obtains from Eq. (6′)

$$\ln P_{S_2}=\tfrac{1}{2}\ln[(1-a)(1-b)(1-c)^2] - \frac{1}{kT}\left[w_1\left(\frac{a^2}{2}+2ab+\frac{b^2}{2}+3c^2-6\right) + w_2\{(a+b)c-2\}+w_3(ab+c^2-2)\right] + C_1(T), \qquad (15)$$

where

$$C_1(T)=\frac{2\varepsilon_V-2\mu^\circ_S(T)}{kT}-2\ln q_S(T). \qquad (16)$$

The free energy per gram-atom in the V–S system is expressed as follows:

$$G=(1-X_S)\mathcal{N}kT\ln\lambda_V+X_S\mathcal{N}kT\ln\lambda_S, \qquad (17)$$

where $\mathcal{N}$ is the Avogardo number. Using Eqs. (3′), (4′), (5′), and (6′), $kT\ln\lambda_V$ and $kT\ln\lambda_S$ are written as

$$\begin{aligned} kT\ln\lambda_V &= kT\ln\frac{a}{1-a} - [2(1-a)w_1+2(1-b)\times(2w_1+w_3)+2(1-c)w_2] + C_2(T)\\ &= kT\ln\frac{b}{1-b} - [2(1-b)w_1+2(1-a)\times(2w_1+w_3)+2(1-c)w_2] + C_2(T)\\ &= kT\ln\frac{c}{1-c} - [2(1-c)(3w_1+w_3) + \{(1-a)+(1-b)\}w_2] + C_2(T) \end{aligned} \qquad (18)$$

and

$$kT\ln\lambda_S=\frac{kT}{4}\ln[(1-a)(1-b)(1-c)^2] - \left[w_1\left(\frac{a^2}{4}+ab+\frac{b^2}{4}+\frac{3}{2}c^2-3\right) + w_2\left\{\frac{(a+b)c}{2}-1\right\} + w_3\left(\frac{ab+c^2}{2}-1\right)\right] + C_3(T), \qquad (19)$$

where

$$C_2(T) = -\varepsilon_V - kT \ln q_V(T) \qquad (20)$$

and

$$C_3(T) = \varepsilon_V - kT \ln q_S(T). \qquad (21)$$

Then the free energy per gram-atom, G, is expressed by

$$\begin{aligned} G = \frac{\mathcal{N}}{a+b+2c+4}[&kT\{a \ln a \\ &+(1-a)\ln(1-a) \\ &+b \ln b + (1-b)\ln(1-b) \\ &+2c \ln c + 2(1-c)\ln(1-c)\} \\ &+w_1\{(1-a)^2 + 4(1-a)(1-b) + (1-b)^2 \\ &+6(1-c)^2\} \\ &+2w_2\{(1-a)+(1-b)\}(1-c) \\ &+2w_3\{(1-a)(1-b)+(1-c)^2\}] \\ &+\mathcal{N}(1-X_S)C_2(T) + \mathcal{N}X_S C_3(T). \qquad (22) \end{aligned}$$

Using the specified values of w_1, w_2, and w_3 and the equilibrium occupancy ratios a, b, and c obtained from Eqs. (10) and (11), the composition dependences of the equilibrium sulfur pressure and the free energy may be obtained for each temperature from Eqs. (15) and (22). The values of $C_1(T)$, $C_2(T)$, and $C_3(T)$ have not yet been estimated rationally. The value of $C_1(T)$ was estimated in such a way that the calculated value of P_{S_2} agreed with the experimental value at the composition $V_{0.80}S$ ($X_S = 0.556$). Equation (22) is expressed as follows:

$$G = G' + \mathcal{N}(1-X_S)C_2(T) + \mathcal{N}X_S C_3(T), \qquad (22')$$

where

$$\begin{aligned} G' = \frac{\mathcal{N}}{a+b+2c+4}[&kT\{a \ln a \\ &+(1-a)\ln(1-a) \\ &+b \ln b + (1-b)\ln(1-b) \\ &+2c \ln c + 2(1-c)\ln(1-c)\} \\ &+w_1\{(1-a)^2 + 4(1-a)(1-b) + (1-b)^2 \\ &+6(1-c)^2\} + 2w_2\{(1-a)+(1-b)\} \\ &\times(1-c) + 2w_3\{(1-a)(1-b) \\ &+(1-c)^2\}]. \qquad (23). \end{aligned}$$

The term, $\mathcal{N}(1-X_S)C_2(T) + \mathcal{N}X_S C_3(T)$, depends only on the composition, while G' depends on the occupancy ratios. Then the free energy term G' in Eq. (23) is adequate for the comparison of the stabilities of different types.

Equations (10) and (11) were solved numerically for 750, 888, 1050, and 1217°C by using the various values of w_1, w_2, and w_3. For a set of w_1, w_2, and w_3 three sets of numerical solutions were obtained which were characterized by the following relations, respectively:

$a < b$, $c \doteqdot 1$ (corresponding to the V_3S_4 type);

$a = b < c \doteqdot 1$ (corresponding to the CdI_2 type);

$a = b = c < 1$ (corresponding to the NiAs type).

The results calculated by using the pairwise interaction energies

$\mathcal{N}w_1 = 5.0$ (kcal/mole)

$\mathcal{N}w_2 = 24.5$ (kcal/mole)

$\mathcal{N}w_3 = 1.5$ (kcal/mole)

are demonstrated in Figs. 5, 6, and 7 as a case in which the experimental results are illustrated relatively well. The equilibrium occupancy ratios calculated for 888°C are shown in Fig. 5 with regard to the atom fraction of sulfur, X_S. The free energy curves, G' vs X_S, calculated from Eq. (23) were found to be unsuitable for illustration, because the gradients of the curves were too steep. Therefore, for convenience, $20X_S$ was

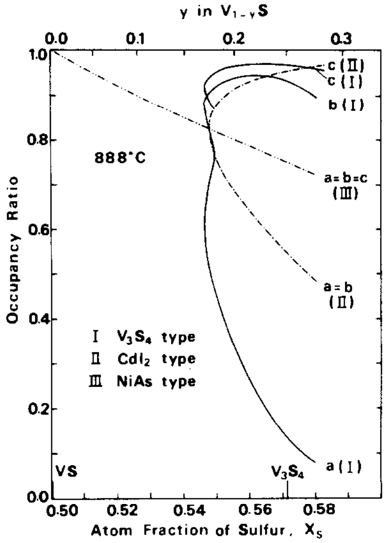

FIG. 5. Equilibrium occupancy ratio vs composition curves calculated from Eqs. (10), (11), and (13) by using the values $\mathcal{N}w_1 = 5$ kcal/mole, (see text). $\mathcal{N}w_2 = 24.5$ kcal/mole, and $\mathcal{N}w_3 = 1.5$ kcal/mole. ——, V_3S_4 type; – · – · –, CdI_2 type; – ·· – ·· –, Ni As type.

subtracted from the value of G' expressed in kcal/mole in order to lay down the curves. The resulting curves, $(G' - 20X_S)$ vs X_S, calculated at 888°C for respective types are shown in Fig. 6a. The curves show that the phases of NiAs type and V_3S_4 type are stable with fairly wide composition ranges and a two-phase region exists as indicated by the common tangent in Fig. 6a. A subtraction of $20X_S$ from the value of G' has no influence on the comparison of the stabilities of respective types and the positions of points of contact such as P and Q in Fig. 6a which indicate the composition of the coexisting phases. The composition dependence of the equilibrium sulfur pressure calculated from Eq. (15) is illustrated in Fig. 6b. The thick solid line on Fig. 6b corresponds to the stable state which changes from the VS type to the V_3S_4 type via the two-phase state. The P_{S_2}–composition curves calculated for 750, 888, 1050, and 1217°C are illustrated together with the experimental results for comparison in Fig. 7.

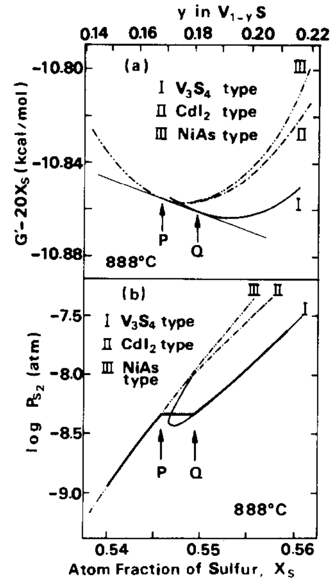

FIG. 6(a) $(G' - 20X_S)$ vs composition curves. G' was calculated from Eq. (23). The common tangent indicates the two-phase region (see text). (b) Composition dependence of the equilibrium sulfur pressure calculated from Eq. (15) (see text).

Qualitatively the experimental results have a trend similar to that of the calculated results at temperatures above 888°C as shown in Fig. 7. That is to say, there is a horizontal part in the P_{S_2}–composition curve which indicates the existence of a two-phase region between the phases near $V_{0.75}S$ and near VS. As the temperature increases, the compositions of both ends of the two-phase region shift to the S-rich side. Accordingly the characteristics of the phase relation of this system in the higher temperature range can be explained on the basis of the model discussed in this paper. Quantitatively, however, considerable differences are recognized as shown in Fig. 7. Satisfactory agreement between the experimental and calculated results has not been obtained in spite of the selection of various values of w_1, w_2, and w_3. At temperatures below 827°C the two-phase region is not found experimentally, contrary to the calculated results which indicate existence of a two-phase

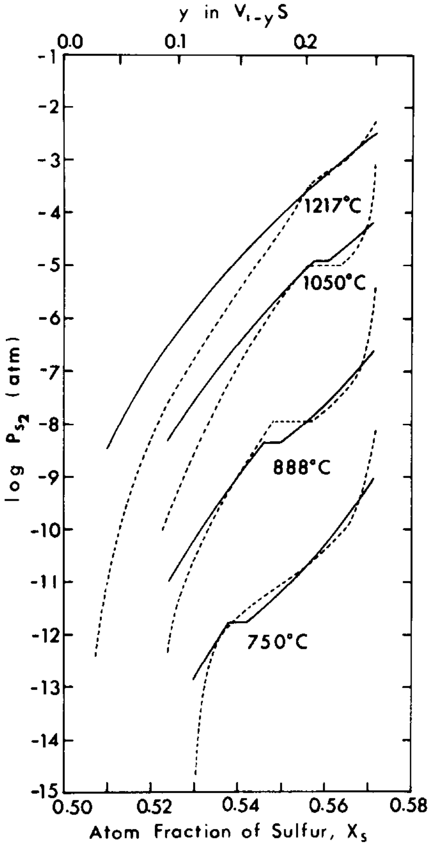

FIG. 7. Calculated and observed equilibrium sulfur pressure curves, ——, calculated; – – –, observed.

region with broader width than those at higher temperatures. This phenomenon is still not interpretable on the basis of the relatively simple model discussed in this paper.

Acknowledgments

The authors thank Drs. I. Kawada, M. Saeki, and K. Shibata for helpful discussion. Thanks are also due to Dr. Y. Onoda for his computer programs.

References

1. F. GRØNVOLD, H. HARALDSEN, B. PEDERSEN, AND T. TUFTE, *Rev. Chim. Minér.* **6**, 215 (1969).
2. A. B. DE VRIES AND F. JELLINEK, *Rev. Chim. Minér.* **11**, 624 (1974).
3. K. SHIBATA, private communication.
4. M. WAKIHARA, T. UCHIDA, AND M. TANIGUCHI, *Mater. Res. Bull.* **11**, 973 (1976); *Met. Trans. B*, **9**, 29 (1978).
5. S. BRUNIE AND M. CHEVRETON, *C. R. Acad. Sci. Ser. C.* **258**, 5847 (1964).
6. M. CHEVRETON AND A, SAPET, *C.R. Acad. Sci. Ser, C* **261**, 928 (1965).
7. S. BRUNIE, M. CHEVRETON, AND J-M. KAUFFMAN, *Mater. Res. Bull.* **7**, 253 (1972).
8. I. KAWADA, M. NAKANO-ONODA, M. ISHII, M. SAEKI, AND M. NAKAHIRA, *J. Solid State Chem.* **15**, 246 (1975).
9. M. NAKANO-ONODA, S. YAMAOKA, K. YUKINO, K. KATO, AND I. KAWADA, *J. Less Common Metals* **44**, 341 (1976).
10. H. NAKAZAWA, M. SAEKI, AND M. NAKAHIRA, *J. Less Common Metals* **40**, 57 (1975).
11. S. HORIUCHI, I. KAWADA, M. NAKANO-ONODA, K. KATO, Y. MATSUI, F. NAGATA, AND M. NAKAHIRA, *Acta Cryst. A* **32**, 558 (1976).
12. Y. OKA, K. KOSUGE, AND S. KACHI, *J. Solid State Chem.* **23**, 11 (1978); **24**, 41 (1978).
13. L. S. DARKEN AND R. W. GURRY, *J. Amer. Chem. Soc.* **67**, 1398 (1945).
14. JANAF Thermochemical Tables, 2nd ed., U.S. Dept. of Commerce, Nat. Bur. Stand., Washington, D.C. (1971).
15. M. KOIWA AND M. HIRABAYASHI, *J. Phys. Soc. Japan* **27**, 808 (1969).